International Journal of Railway Research, (2014), Vol.1, No2, pp 59-73 ISSN: 236153768187

Iran University of Science and Technology

International Journal of

Railway Research

Study on new crashworthy buffers in railway

Amirsaeed Hosseini, Parisa Hosseini Tehrani *

Center of excellence in railway transportation, School of Railway Engineering, Iran University of Science & Technology, Tehran 16846-13114, Iran

ABSTRACT

At the collision time, a lot of energy is generated during a short period of time that causes large deformations in bodies. One of the most important parts of wagon in railway is a buffer which may absorb the energy during an impact. It should be mentioned that normal buffers only absorb the energy resulted from a crash elastically. In the present paper, it is tried to use inversion mode of deformation in cylindrical tube, in order to improve energy absorption of new design buffers through plastic deformation, in addition to elastic energy absorption. On the other hand during sever impact the improved buffers may enter plastic phase and absorbs some of the energy generated by impact in this phase after being deformed elastically. The main structure of buffers is composed of cylindrical tubes which can prevent deformation of important structures such as wagons through being deformed at the impact time. One of the most stable and practical modes of energy absorption for cylindrical tube in plastic state is inversion. In this paper, inversion is used to increase the amount of energy absorption in railway buffers. In addition, the features of force–displacement curves, energy–displacement curves, and deformation modes are analyzed by using the non-linear finite element code LS-DYNA.

Keywords: Railway buffer, cylindrical tubes, Energy absorption, Inversion, LS-DYNA

1. Introduction

One of the most important parts of wagons for preventing shock during an impact is buffer. The buffers are constituted of two types of tubes which are inserted inside each other. The outer tube is fixed while the internal tube is sliding. In Fig. 1 the schematic presentation of a buffer is displayed.

The main duty of the buffers is absorbing or reducing the energy which is generated during several impacts, which may occur between adjacent wagons, with different angles. Energy absorption is mostly elastic in normal buffers. In the present work, it is tried to add plastic deformation to the normal buffers in order to increase the amount of energy absorption of the buffers.

The thin-walled tubes are very effective in absorbing kinetic energy resulted from collision in different vehicles including airplanes, automobiles, and trains. Thin-walled tubes can be used in different ways as energy absorbers [1,2]. Abramowicz and Wierzbicki obtained the mean crushing force for square tubes by developing a simplified model based on rigid plastic assumptions [3]. By taking account of strain-rate and effective crushing distance, the collapse model were modified [4,5]. Researchers concentrated on the crushing characteristics of aluminum alloy and steel square tubes.[6,7]. In addition, the behavior of tubular structures during crushing was studied by Alghamdi

*Corresponding Author
Email Address: hosseini_t@iust.ac.ir

[8]. The effects of geometry, material properties, and boundary conditions on the axial crushing of thin-walled tube were studied by Jensen et al. [9]. Dynamic effects of axial crushing of square tubes were studied in [10,11]. Moreover, the researchers concentrated on the external inversion of thin-walled tubes over the past years. Reddy and Reid identified the main process parameters [12,13]. Recent work which is about the prediction of the load-displacement curve and it was based on finite element analysis was studied by Yang et al. [14]. Also the geometrical features of tubes and dies were studied by Sekhon et al. [15]. Furthermore, Martins et al. studied the influence of interface friction on the material flow [16]. Since inversion is one of the most stable and predictable method of energy absorption in cylindrical and thin walled tubes this method is examine to design a crashworthy buffer in this task. To achieve this goal, different arrangement of cylindrical tubes have been used and studied under different impact angle in buffers.

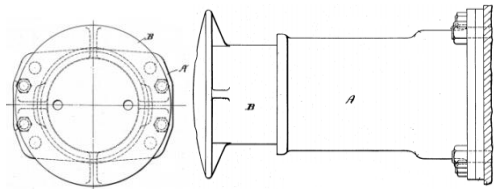

Figure 1. The schematic representation of a railway buffer

2. External inversion

In external inversion, the lower jaw is fixed while the upper jaw is crushed with the tube in static mode. The curvature radius of die is r_{cd} and the thin-walled tube is crushed with the constant velocity (V). The parameters such as thickness of tube (t_0) and curvature radius of the die (r_{cd}) are important factors in external inversion of the thin-walled tubes [17]. In Fig. 2, the schematic presentation of external inversion is shown.

To be certain about the responses obtained from LS-DYNA for railway buffers, at first, the simulation on a thin-walled tube made of aluminium alloy Al6060 with a density of 2700 Kg/m^3 and Young modulus E= 70 Gpa, with a stress-strain curve shown in Fig. 3 is considered. The length of tube (l_0), thickness (t_0), and radius of die curvature (r_{cd}) for the thin-walled tube are 70mm, 2mm, and 5mm, respectively [17].

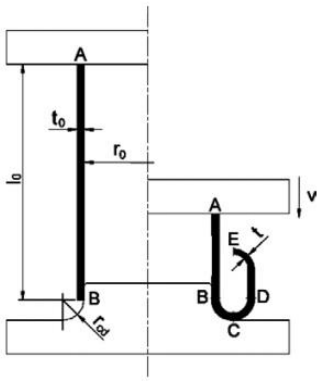

Figure 2. The schematic presentation of external inversion [17]

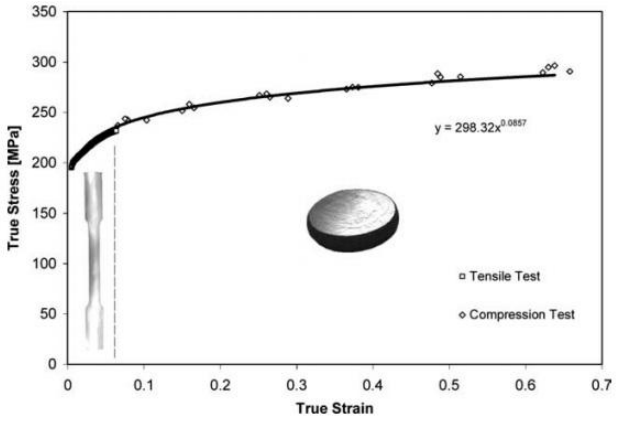

Figure 3. Stress-strain curve of the Al6060 aluminium alloy obtained by tensile and compression tests [17]

In the present simulation, the ratio of $r_{cd}/r_0 = 0.278$ for a successful external inversion is considered. It should be mentioned that, the local buckling is observed in values less than $r_{cd}/r_0=0.21$, while for values more than $r_{cd}/r_0 = 0.42$ a local crack is created in the tube. Both of these situations are undesirable and in this case, the ability of tube for absorbing energy is reduced [17]. Fig. 4 illustrates the crush simulation of aluminium tube in LS-DYNA.

The stages of thin-walled tube deformation due to external inversion after crush are displayed in Fig. 5.

The results obtained from the software and the ones gained from experimental data compared in Fig. 6. According to Fig. 6, there is a good compatibility of

experimental results and the results obtained from LS-DYNA.

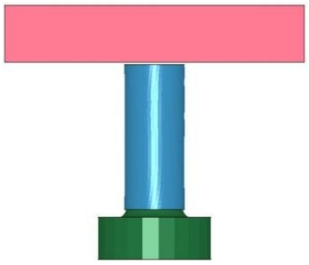

Figure 4. Simulation of aluminium tube collision

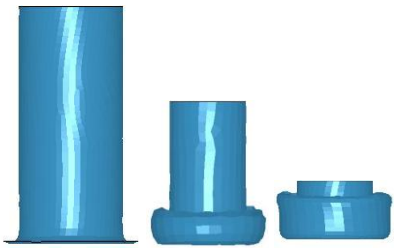

Figure 5. The stages of deformation of aluminium tube due to external inversion

shell elements with five integration points through the thickness. All tubes are meshed with quadrilateral elements [18]. A rigid plate with a mass of 80 tons as the wagon is collided with buffer in a constant velocity of 10 km/h [19]. The material of all the tubes and rigid parts of buffer used here is 1018 steel with the following mechanical properties: Young modulus E = 200 GPa, initial yield stress σ_y=310 MPa, tangent modulus E_T = 763MPa, ultimate tensile stress σ_u = 504 MPa, density ρ=7865 kg/m3, and Poisson's ratio υ = 0.27 [20]. Plastic kinematic model is employed to simulate tube materials. Self-contact interaction is simulated using an "automatic single surface" to the part of thin-walled tube to avoid interpenetration of tube wall. To account for contact between the rigid bodies and tubes, "node to surface" and "automatic surface to surface" contacts are defined. Strain rate effect is included using the Cowper and Simonds model. Cowper and Symonds strain rate parameters C and q for 1018 steel are 40 (s^{-1}) and 5, respectively [20]. The static and dynamic coefficients of friction for all surfaces are 0.2 [20]. The whole free length of the usual buffer is 620mm [24]. Furthermore, a buffer

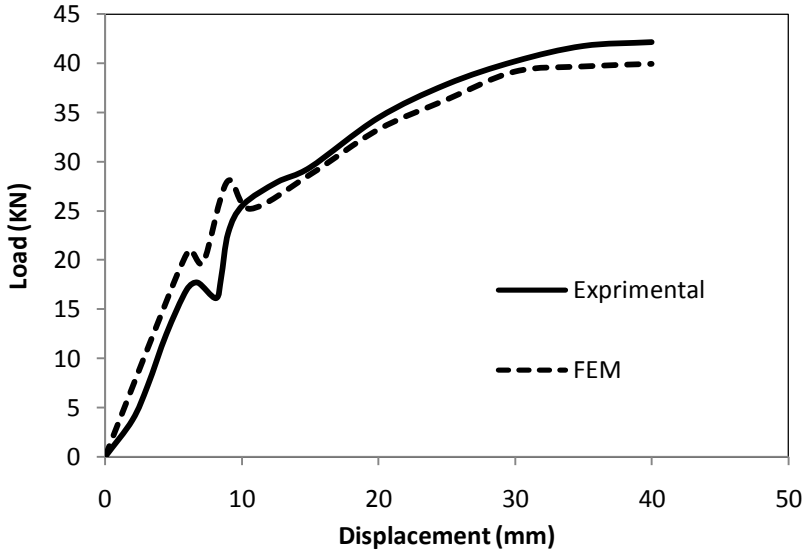

Figure 6. Comparison between the results obtained from [17] and LS- DAYNA

3. Finite element modeling

The explicit non-linear finite element code LS-DYNA was used to predict the responses of buffers subjected to axial and oblique crashing. The sidewall of tubes is modelled with Belytschko-Tsay four-node spring which can absorb the impact energy of 30 KJ in elastic phase is used [19].

The elastic deformation of the buffer spring is 110mm, while total compression, which includes elastic deformation and non-reversible deformation in

plastic phase, is considered at least 160 mm [19] .The positions of buffer spring and other components of railway buffer are shown in a schematic representation in Fig. 7. It should be pinpointed that, in addition to axial crash, the impact with different oblique angles (θ = 0^o, 5^o, 10^o) have been studied too. The angle of θ is shown in Fig. 12.

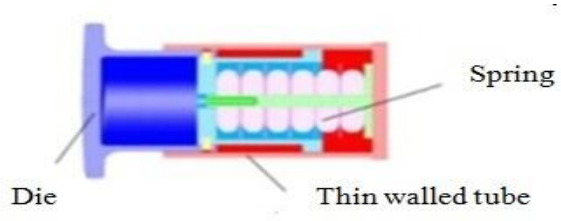

Figure 7. The components of railway buffer [25]

4. Finite element model in axial collision mode

In Fig. 8, a general schematic presentation of buffer simulation in LS-DYNA during an axial crash (θ= 0^o) is shown.

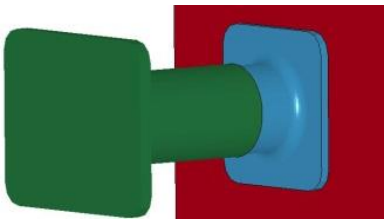

Figure 8. General schematic presentation of buffer simulation in axial mode (θ= 0^o)

In this section, external inversion occurs for thin-walled tube with a thickness of 9mm [18]. According to [17], one of the appropriate ratios for r_{cd}/r_0 which is r_{cd}/r_0 = 0.278 is applied for a successful external inversion. The internal radius of thin-walled tube (r_0) is about 100mm [19], therefore, the radius of the die curvature is considered r_{cd}=27.8 mm. The deformed model of buffer after successful external inversion is illustrated in Fig. 9.

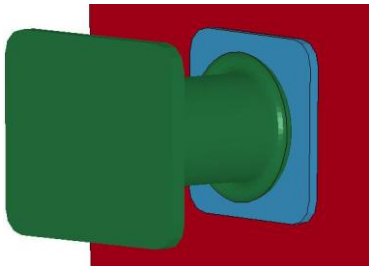

Figure 9. Buffer deformation after external inversion in axial collision mode (θ= 0^o)

The diagram of force-displacement for the deformed tube after external inversion in axial collision is shown in Fig. 10. The distance of the rigid wall with the buffer is considered 90 mm, so that the total displacement of the rigid wall after the elastic deformation of the spring and maximum plastic deformation of buffer's cylinder is 250 mm in axial collision which is shown in Fig. 10.

Fig. 11 is about the diagram of energy-displacement for the thin walled tube of buffer during the axial impact. It should be stated that in this diagram just the impact energy which is absorbed by thin-walled tube in

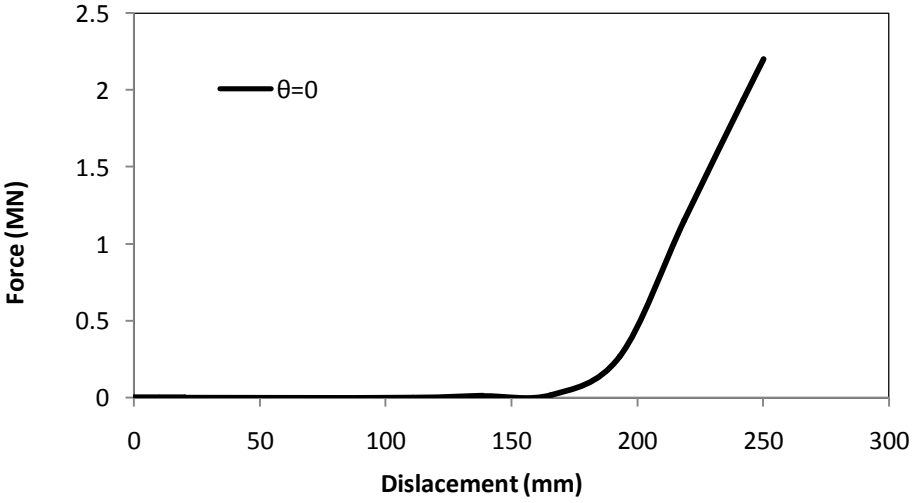

Figure 10. The diagram of force-displacement in axial collision mode (θ= 0^o)

the buffer is considered. Hence, the energy absorption by the spring, which is about 30 KJ, should be added to the value of energy absorption in plastic phase.

mode. The buffer deformation model after external inversion with $\theta=10^o$ is illustrated in Fig. 13.

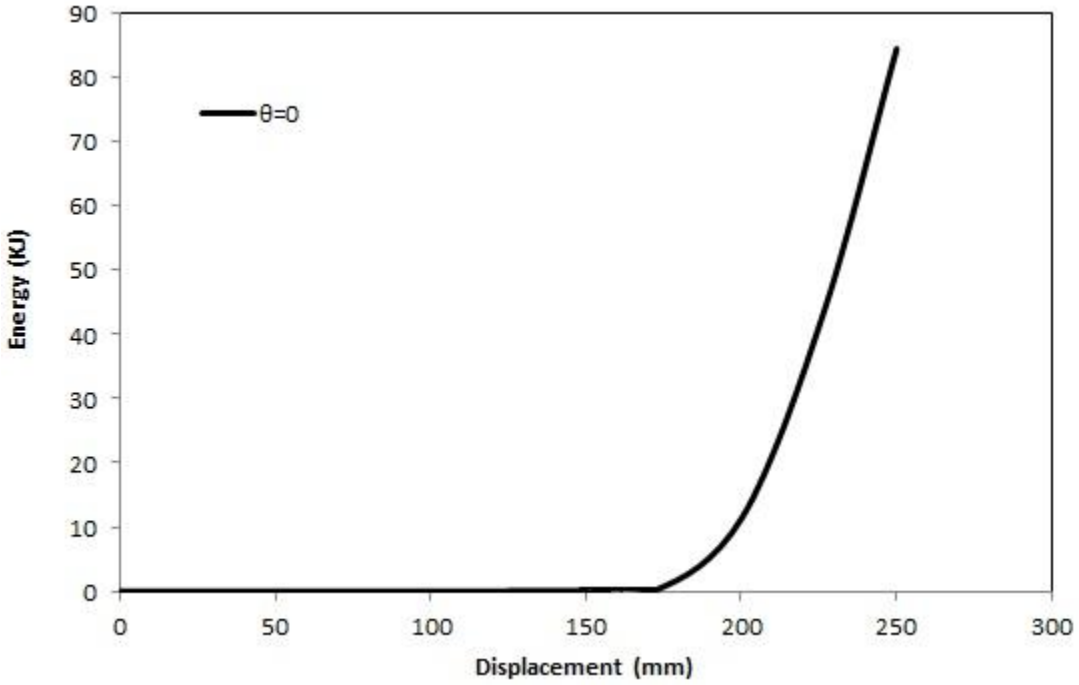

Figure 11. The diagram of energy-displacement in axial collision mode ($\theta= 0^o$)

5. Finite element model in oblique impact

In this section, the oblique impact with different angels is considered ($\theta = 5^o, 10^o$). For example, In Fig. 12, the general schematic presentation of buffer simulation in the impact with an oblique angle of 10 ^{o} in LS-DYNA is illustrated.

These angles ($\theta = 5^o, 10^o$) are achieved by rotating the rigid wall representing the wagon around one of its axis, so that the displacement of the rigid wall is reduced in comparison to the axial collision as is shown in Fig. 14. In addition, oblique collision leads to increase the amount of energy in the beginning of the displacement of the rigid wall compared to the axial collision. It should be noted that the velocity of the rigid wall is considered 10 Km/h in the oblique collisions too.

The external inversion in oblique impact occurs for the thin-walled tube with a thickness of 9mm [20]. Parameters such as thickness and the radius of die curvature are considered similar to the axial collision

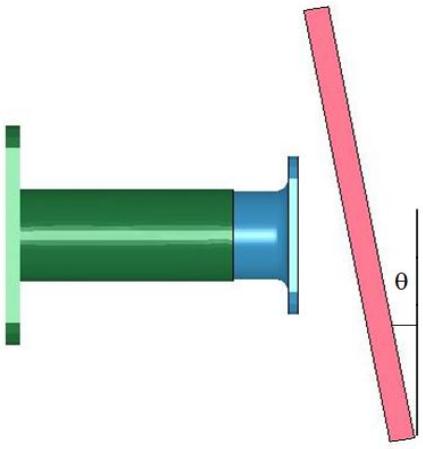

Figure 12. General schematic presentation of buffer in eccentric collision with a collision angle of $\theta=10^O$

The diagram of force-displacement for the deformed thin-walled tubes after external inversion with different angels ($\theta= 0^o, 5^o, 10^o$) is shown in Fig. 14. It should be noted that in this paper, for all of the crash simulation of buffers, the impact velocity of 10 Km/h is considered. All of the curves for force – displacement and energy – displacement diagrams are started from

zero, since in the beginning of the crash there is a gap between rigid wall and the buffer. After that the amounts of force and energy increase as it shown in Fig. 14, 15 till the buffer spring is deformed up to 160 mm which is total amount of elastic and plastic deformation.

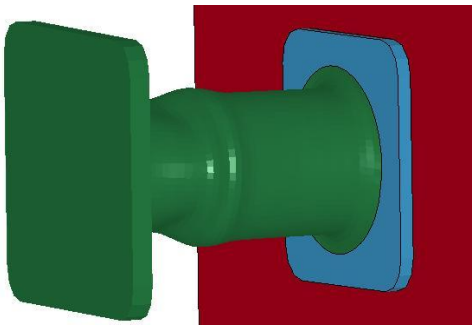

Figure 13. Buffer deformation model after external inversion in eccentric collision mode ($\theta=10^o$)

Fig. 15 shows that the most amount of energy during the impact is absorbed in the oblique impact mode ($\theta=10^o$) which is about 165 KJ. In addition, in the angles of $\theta=0^o$ and $\theta=5^o$, the amounts of energy absorption are 114 KJ and 135 KJ, respectively. The rate of energy absorption increases by increasing the oblique angles up to $\theta=10^o$, and this is due to local buckling which was occurred during the oblique impact that caused to increase the amount of energy absorption in addition to the external inversion mode. The local buckling of tubes is shown in the Fig. 13.

6. Retractable buffers

For inversion with a die, there are some limitations such as using an especial die with a specific relation between the dimensions of tube and die. In addition, as is illustrated in Fig. 16 the short crushing distance feature in inversion with a die, which is about half of the initial length of the tube, is unsatisfactory [20].

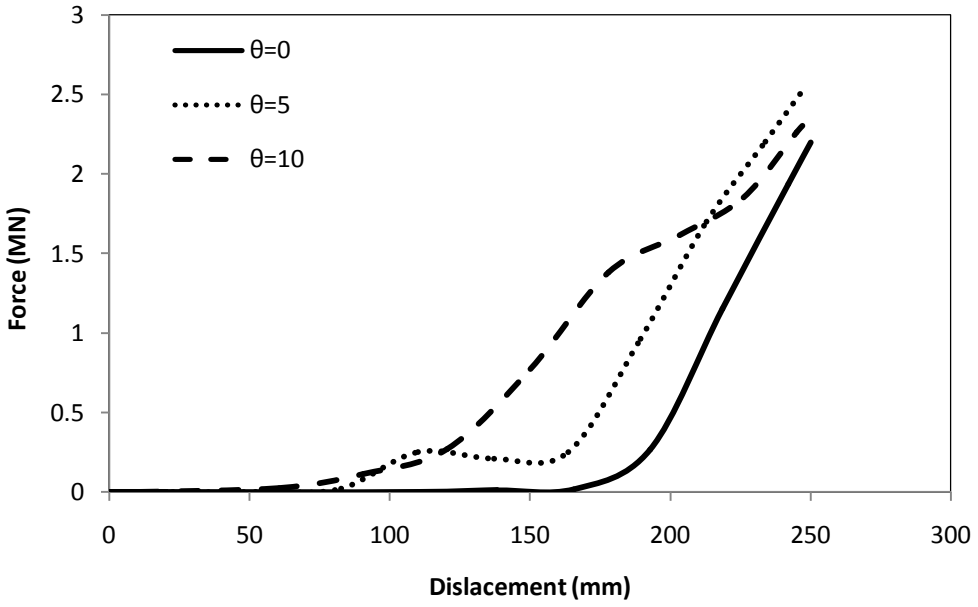

Figure 14. The diagram of force-displacement in eccentric collision mode

Fig. 15 is about the diagram of energy-displacement for the deformed buffers after external inversion with different angels ($\theta=0^o$, 5^o, 10^o). It should be mentioned that these diagrams are about energy absorption of thin-walled tubes of buffers in plastic phase and the energy absorption in elastic phase by the buffer spring which is about 30 KJ should be added to these values.

Besides short crushing distance feature in inversion with a die, short elastic displacement of buffer spring led to use of a new type of structure based on the free inversion of circular tubes which are called retractable tubes. For these kind of energy absorbers, no attachments are needed and long crushing distance can

be achieved. The structure is constituted by cylindrical tubes as shown in Fig. 17(a), or can be formed by combination of cylindrical tubes and tapered tubes as given in Fig. 17(b). The former structure is called straight retractable (SR) tube and the latter is named tapered retractable (TR) tube. For SR tubes, the lower cylinder tube has a big diameter and the length of the upper tube is designed to be twice that of the lower tube in order to obtain high crushing distance up to two third of the whole length. In addition, since for the TR tube, the upper tube is predicted to have a higher inversion load, the length of the lower tube is twice that of the upper tube [20].

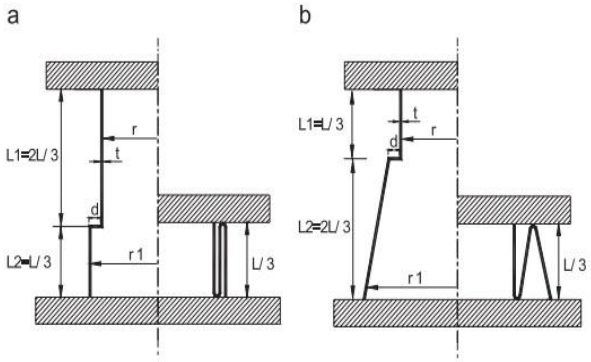

Figure 17. Scheme of retractable tube: (a) SR tube and (b) TR tube [20]

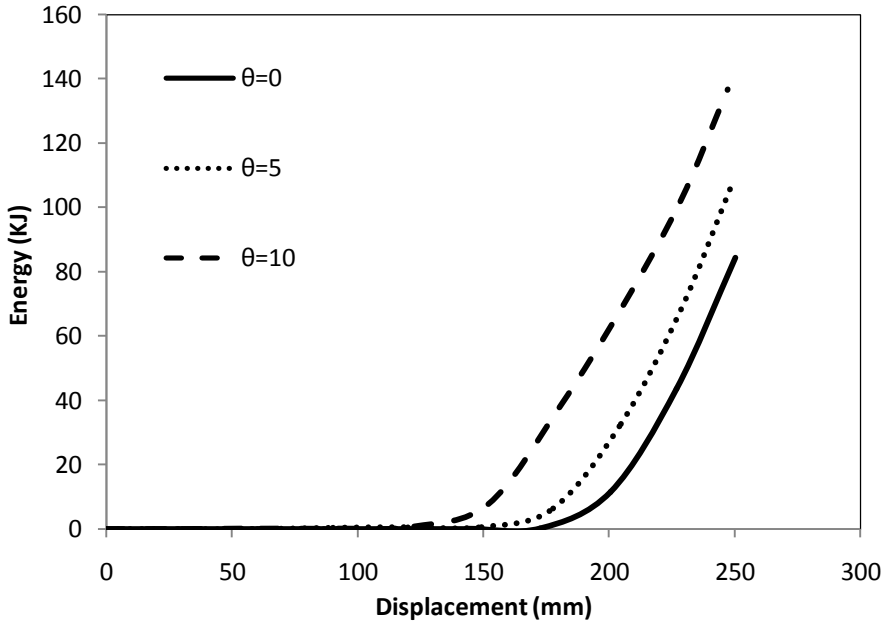

Figure 15. The diagram of energy-displacement in eccentric collision mode

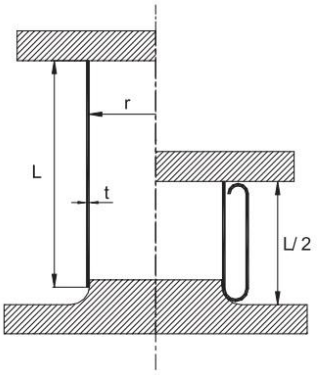

Figure 16. Crushing distance of inversion with a die [20]

In this paper, we use these kinds of new energy absorbers as railway buffers. At the first, SR and TR tubes are considered as energy absorbers in railway buffers, separately. Finally, a combination of SR and TR tubes are formed as a railway buffer, in order to improve the impact characteristics of these energy absorbers. Also the differences of using each kind of these retractable tubes in railway buffers are discussed. It should be noted that, the crashes in SR and TR tubes, are considered in different impact angles ($\theta = 0^o, 5^o, 10^o$).

7.1 SR buffers

The finite element model of SR buffers during axial impact and the position of the spring are shown in Fig. 18. It should be mentioned that the length of the thin-walled tube in retractable buffer is considered about 800 mm [18], and the collision modes in different impact angles are occurred in the impact velocity of 20 Km/h. This incensement of the buffer length provide a deformation stroke independent of spring deformation of the buffer and leads to more plastic deformation of the railway buffer and absorbing more amount of energy. In these buffers, the spring deforms in its total distance, but the deformation of the thin-walled tube may be continued without any limitation due to buffer spring.

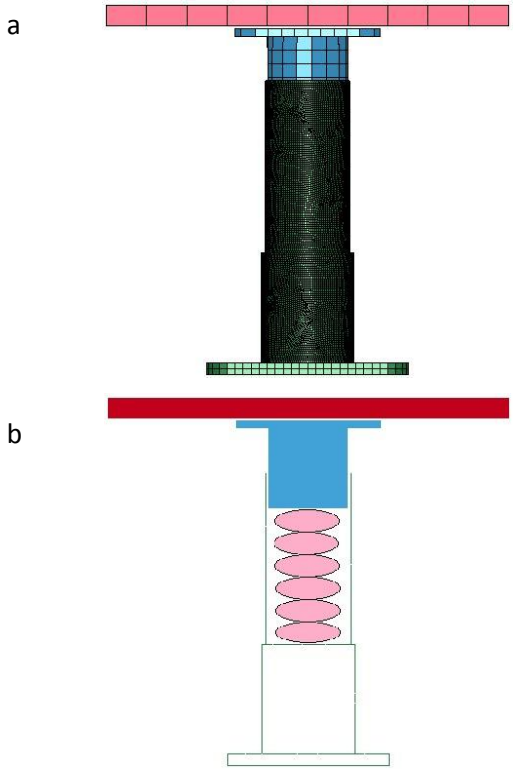

Figure 18. (a) Finite element model of SR buffer (b) Cross section SR buffer

The spring is positioned in the upper tube and after elastic deformation of the buffer, plastic deformation in internal inversion mode occurs in the lower tube of the SR buffer. Retractable buffers cause more crushing distance in comparison to buffers which were discussed in section 5. The final deformation of SR buffer during axial impact is shown in Fig. 19.

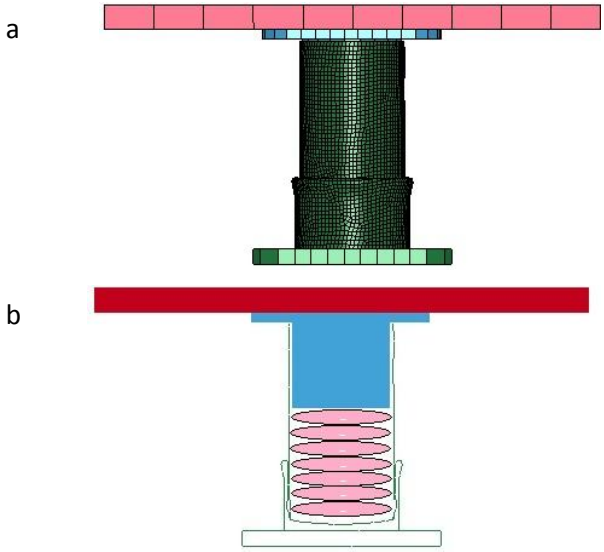

Figure 19. (a) Finite element model of deformed SR buffer ($\theta= 0^o$) (b) cross section of deformed SR buffer ($\theta= 0^o$)

The deformed shapes of SR tubes after collision in different impact angles are shown in Fig. 20.

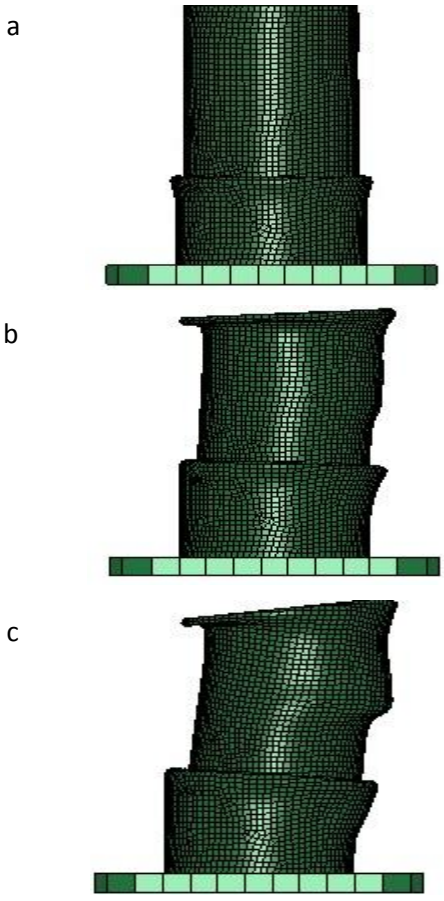

Figure 20. The deformed shapes of SR buffers during different collision angles (a) $\theta= 0^o$ (b) $\theta= 5^o$ (c) $\theta= 10^o$

Fig. 21 and 22 are about the diagrams of force-displacement and energy- displacement for the thin-walled tube of SR buffers during different impact angles. As is illustrated in Fig. 22 the amount of energy absorption is in SR tubes during different impact angles in plastic phase are about 437, 441, and 468 KJ, respectively. Also the overall amounts of energy in both elastic and plastic phases are about 467, 471, and 498 KJ.

7.2 TR buffers

The finite element model of TR buffers during axial impact is shown in Fig. 23. Since we want to use TR buffer in the outer tube of railway buffers in the combined TR and SR energy absorber, and in order to compare TR tubes with the combination model the elastic spring is not used in TR buffers. As it is shown an internal inversion is occurred in the lower tube,

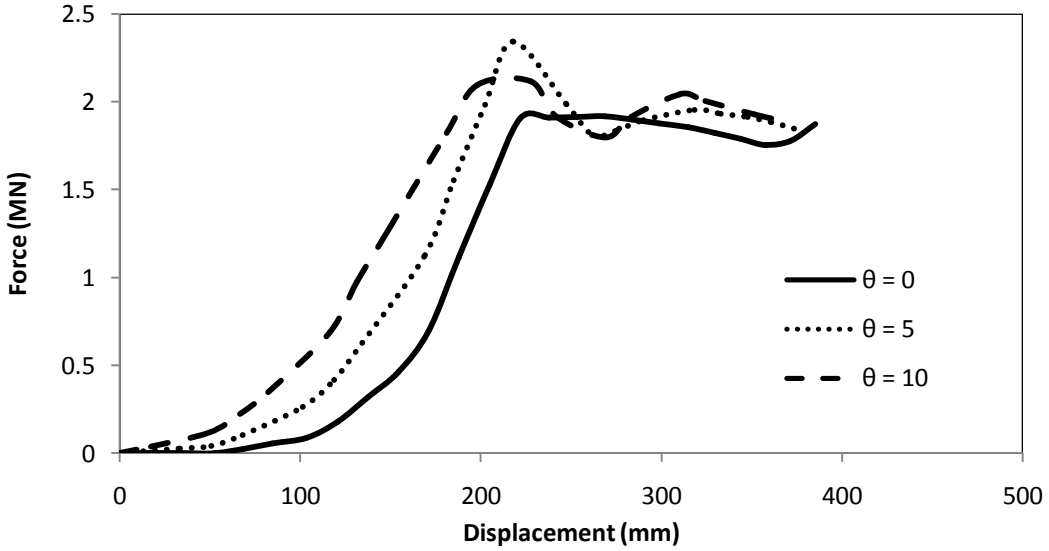

Figure 21. The diagram of force- displacement for SR buffers in different collision angles ($\theta = 0^o, 5^o, 10^o$)

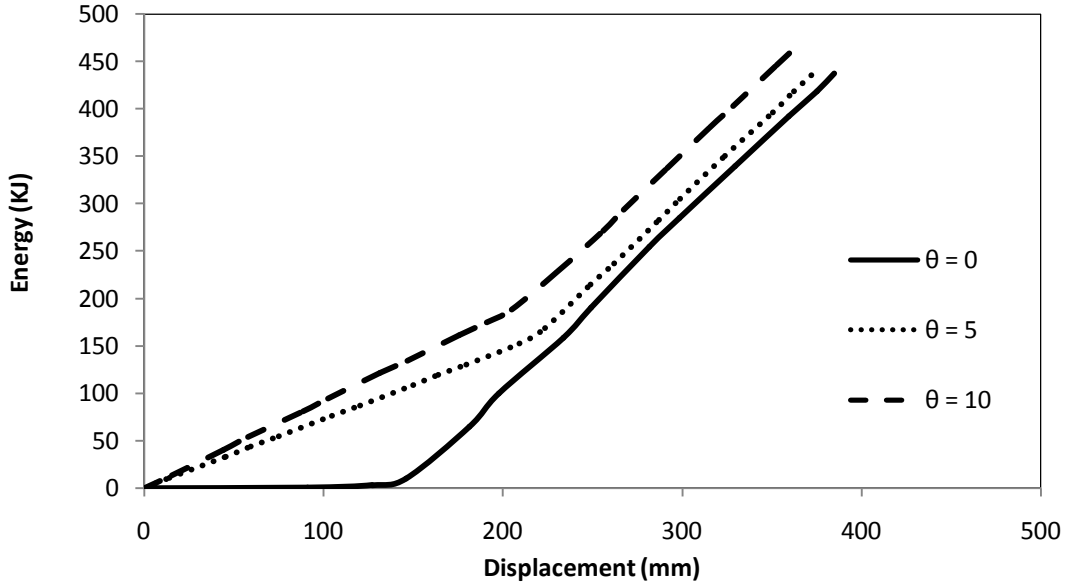

Figure 22. The diagram of energy- displacement for SR buffers in different collision angles ($\theta = 0^o, 5^o, 10^o$)

while there is an external inversion in the upper tube. Since there is no elastic spring in the TR tube which caused some limitations in SR tubes, these two kinds of inversions in TR buffers lead to absorb more amount of energy in comparison to the SR buffers. The collision modes in different impact angles are occurred in the impact velocity of 20 Km/h.

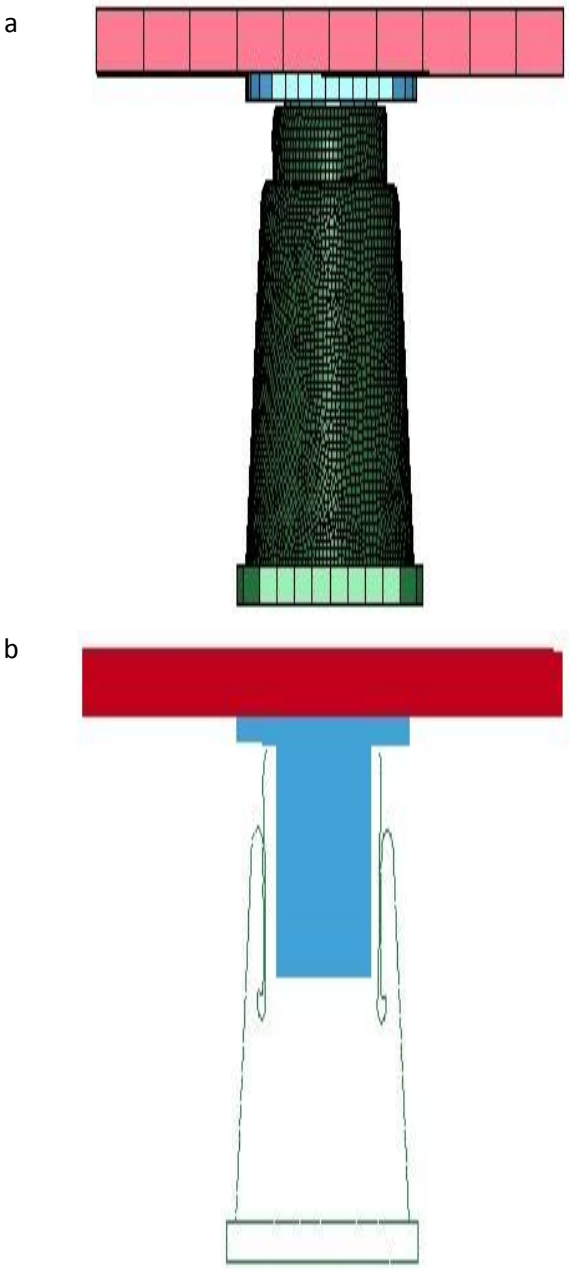

Figure 23. (a) Finite element model of deformed TR buffer ($\theta= 0^o$) (b) Cross section of deformed TR buffer ($\theta= 0^o$)

The deformed shapes of TR buffers after collision in different impact angles are shown in Fig. 24.

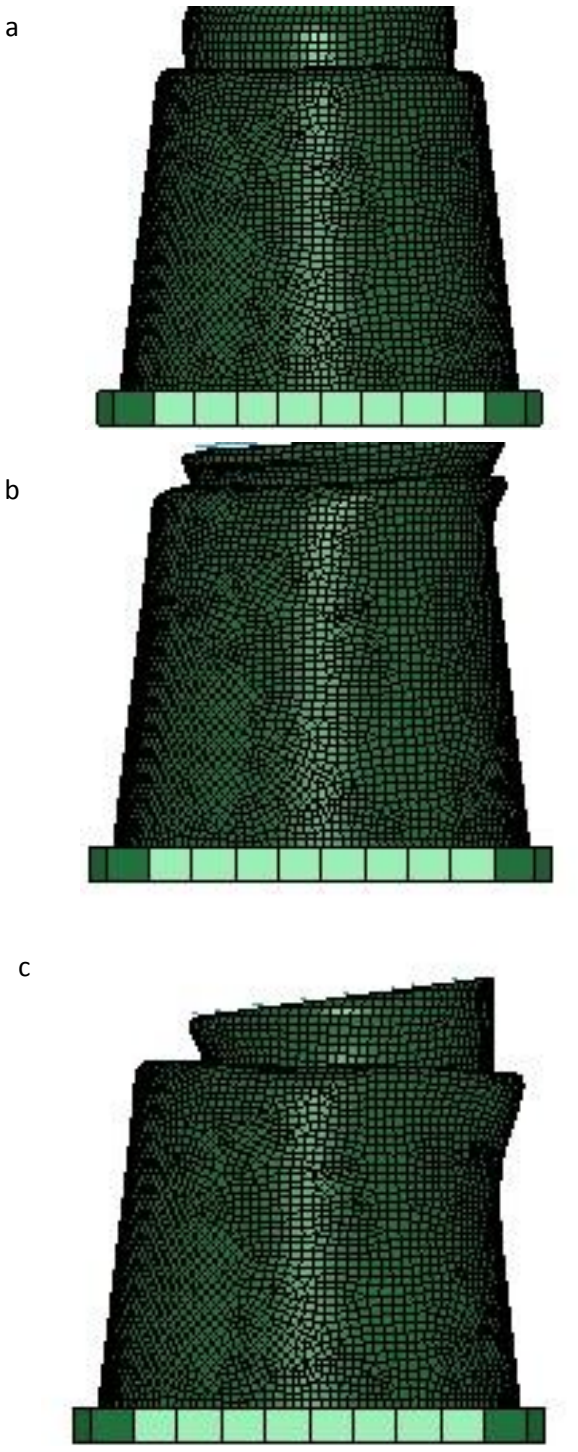

Figure 24. The deformed shapes of TR buffers during different collision angles (a) $\theta= 0^o$ (b) $\theta= 5^o$ (c) $\theta= 10^o$

Fig. 25 and 26 are about the diagrams of force-displacement and energy- displacement for the thin-walled tube of TR buffers during different impact angles. As is illustrated in Fig. 26 the amount of energy absorption is in TR tubes during different impact angles in plastic phase are about 372, 393, and 396 KJ,

respectively. Conclusively, the total amounts of energy are about, 402, 323, and 426 KJ, respectively.

tube and the outer tube of energy absorber is formed of TR tube. As is illustrated, there are two modes of

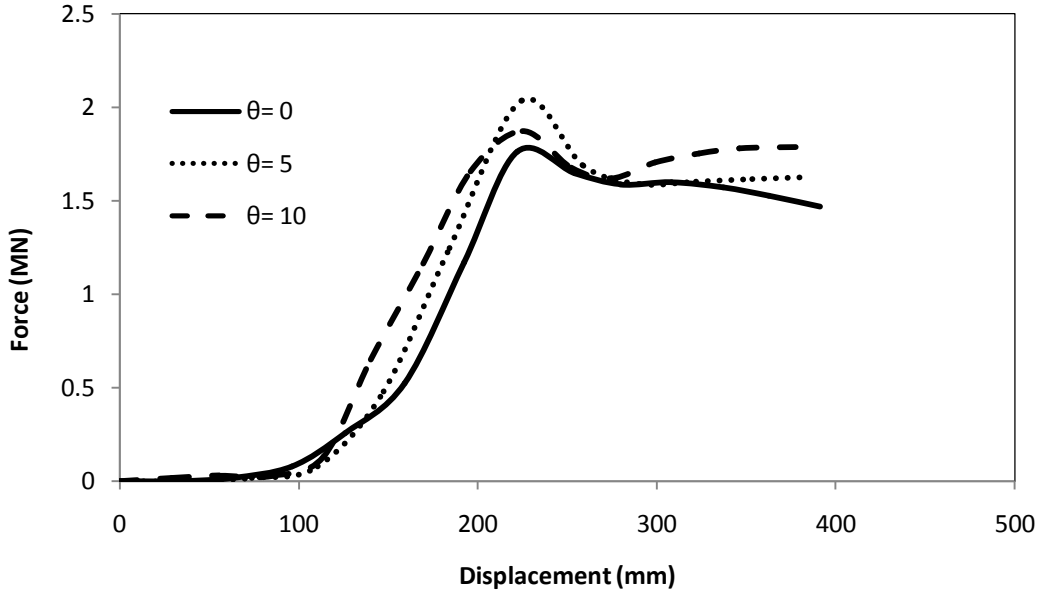

Figure 25. The diagram of force- displacement for TR buffers in different collision angles ($\theta= 0^o, 5^o, 10^o$)

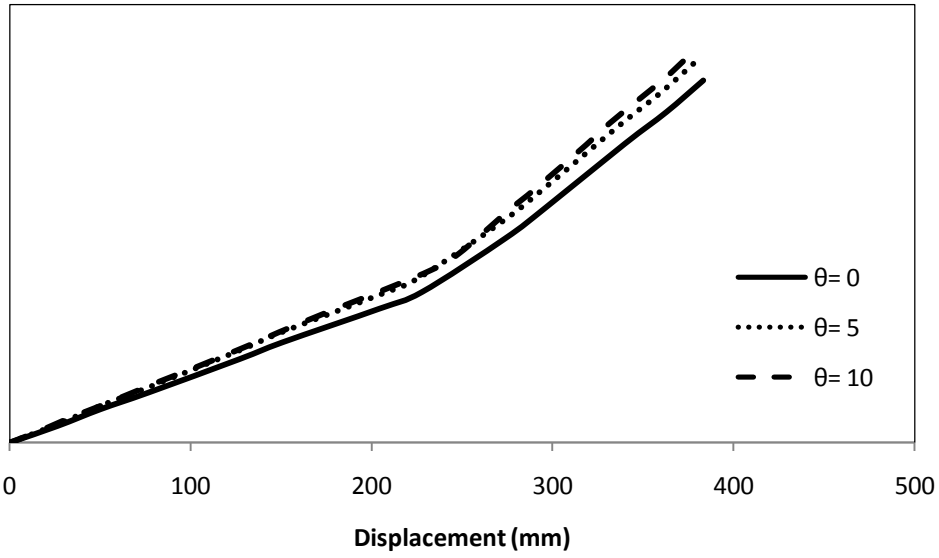

Figure 26. The diagram of force- displacement for TR buffers in different collision angles ($\theta= 0^o, 5^o, 10^o$)

7.3 Combines SR and TR buffers

The finite element model of the combination of SR and TR tubes during axial impact is shown in Fig. 27. The inner tube of railway buffer is considered as SR

internal inversion in SR and TR tubes, and also there is one mode of external inversion in TR tube. Because of this combination of SR and TR tubes, the amount of energy absorption in this new kind of buffer is increased in comparison to SR and TR tubes, separately. However, the amount of pick force is

increased in this new kind of buffer in comparison to SR tube and TR tube, separately. The amount of peak force in the combination form is about 3.63, 4.34, and 4.06 MN, respectively The collision modes in different impact angles are occurred in the impact velocity of 20 Km/h.

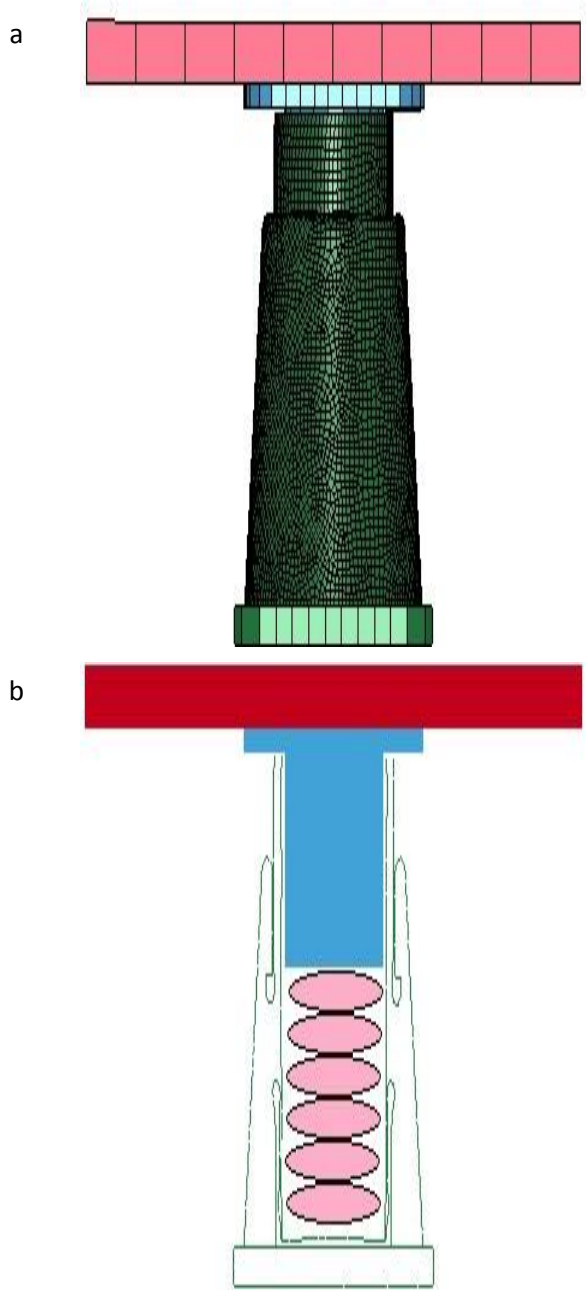

Figure 27. (a) Finite element model of deformation of combined SR andTR buffer ($\theta= 0^o$) (b) cross section of cobined SR and TR buffer ($\theta= 0^o$)

The deformed shapes of combined TR and SR tubes after collision in different impact angles are shown in Fig. 28.

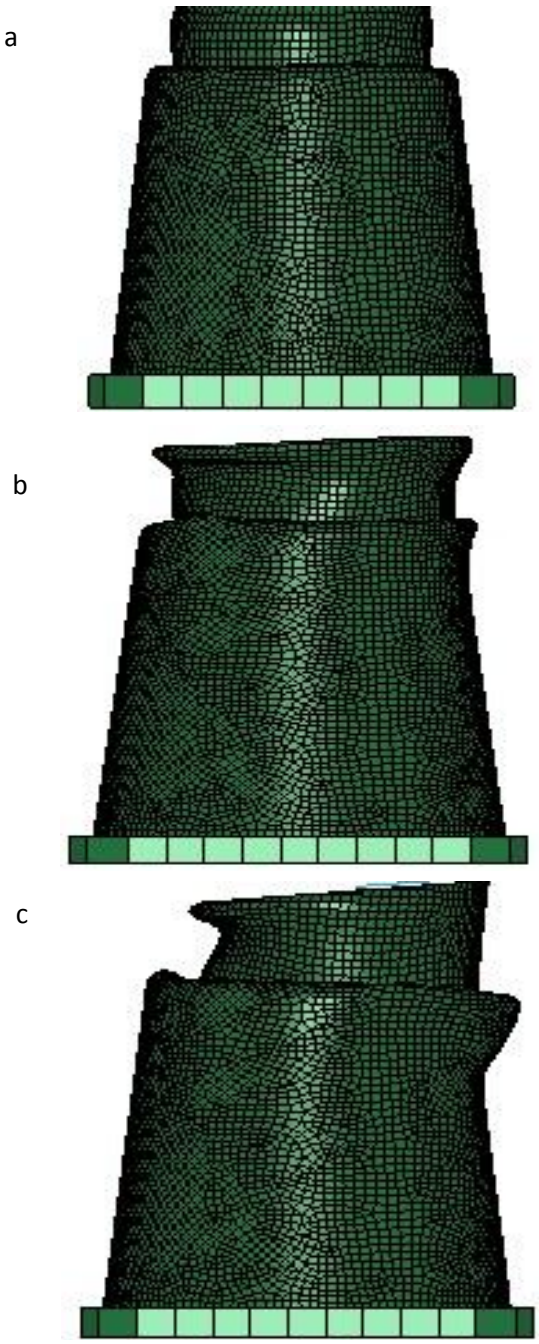

Figure 28. The deformed shapes of combined SR and TR buffers during different collision angles (a) $\theta= 0^o$ (b) $\theta= 5^o$ (c) $\theta= 10^o$

Fig. 29. And 30 are about the diagrams of force-displacement and energy- displacement for the thin-walled tube of combined TR and SR buffers during different impact angles. As is illustrated in Fig. 30 the amount of energy absorption is in combination mode during different impact angles in plastic phase are 717, 841, and 857KJ, respectively. Also the overall amount of energy in both elastic and plastic phases are about 747, 871, and 887 KJ.

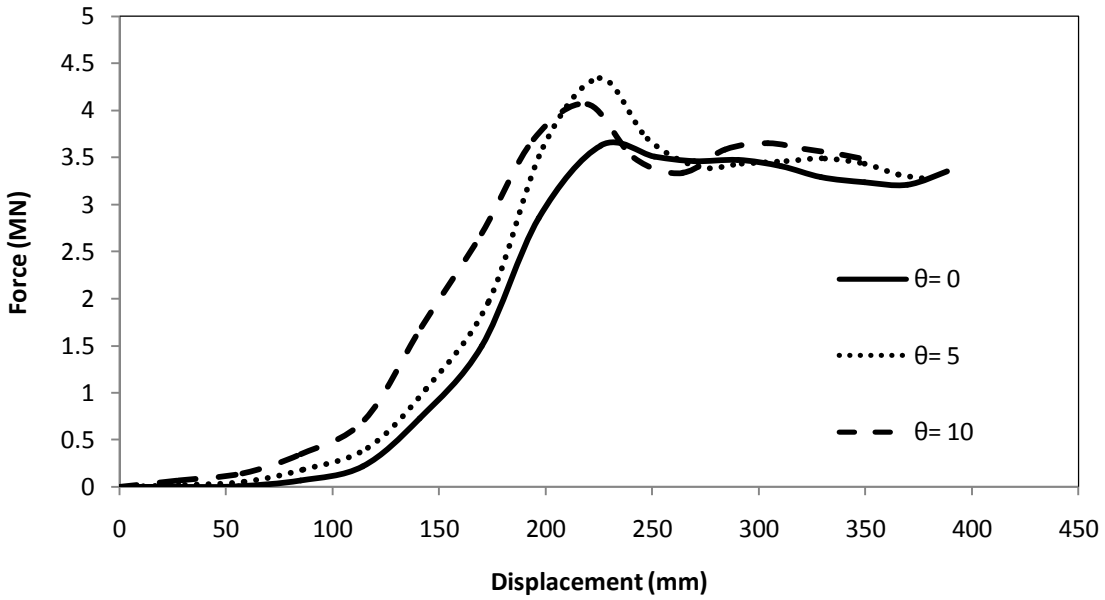

Figure 29. The diagram of force- displacement for combined SR and TR buffers in different collision angles (θ= 0°, 5°, 10°)

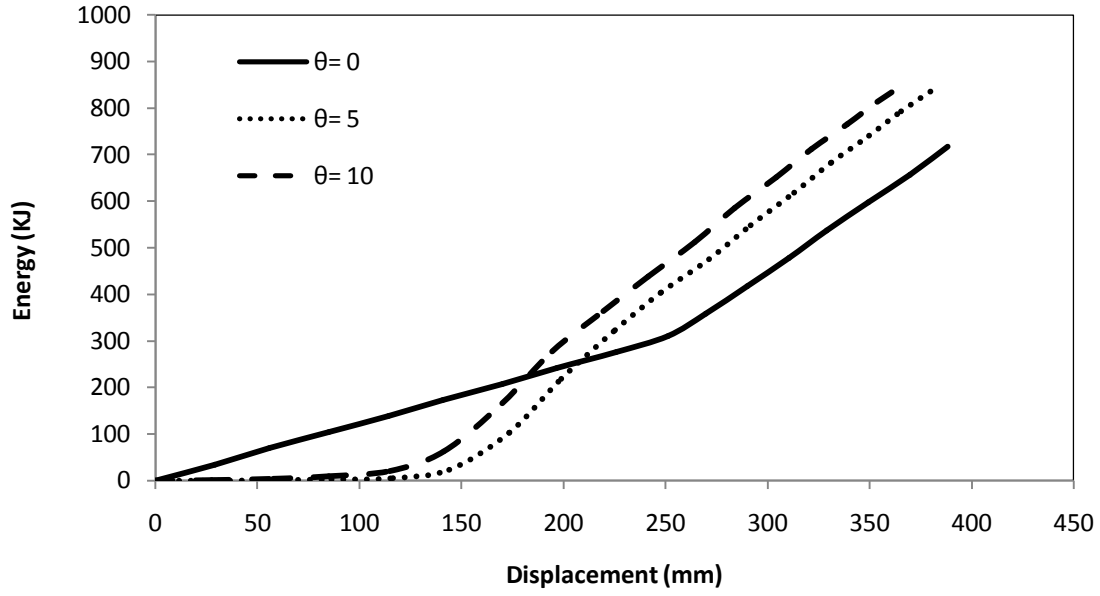

Figure 30. The diagram of energy- displacement for combined SR and TR buffers in different collision angles (θ= 0°, 5°, 10°)

7. Conclusions

In this paper, the effects of using inversion in railway buffers, during axial and oblique loading with different collision angles, is studied. In these phenomena, the ratio of r_{cd}/r_0, i.e., the ratio of radius of die curvature to the internal radius of thin-walled tube for a successful external inversion is necessary. At the time of axial collision in usual buffer, the total absorbed energy is about 114KJ, while, this value is several times of the absorbed energy by buffer spring in

elastic mode. Furthermore, the values of absorbed energy in eccentric collision for $\theta = 5^o$, 10^o are about 135 KJ and 165 KJ, respectively.

Besides short crushing distance feature in inversion with a die, short elastic displacement of buffer spring led to use of a new type of structure based on the free inversion of circular tubes which are called retractable tubes. For these kinds of energy absorbers, no attachments are needed and long crushing distance can be achieved. In this paper, we used these kinds of new energy absorbers as railway buffers. At the first, SR tubes and TR tubes were considered as energy absorbers in railway buffers, separately. Finally, a combination of SR and TR tubes were formed as a railway buffer, in order to improve the impact characteristics of these energy absorbers. Also the differences of using each kind of these retractable tubes in railway buffers were discussed. As it is shown, the amounts of energy absorption in combined mode during different impact angles in plastic phase are 717, 841, and 857KJ. Also the overall amounts of energy in both elastic and plastic phases are about 747, 871, and 887 KJ. In addition, in the new buffer design, more crushing distance is provided in comparison to the external inversion mode in normal railway buffers. Therefore, the amount of energy absorption can be augmented by two ways. First of all by obtaining high crushing distance during an impact and then by using more cylindrical structure in comparison to normal buffers.

It is shown that the new presented buffer has a good stability under oblique loading that may occur in wagons buffer. from the force displacement carves it is seen may be seen that under nearly constant peak force the great amount of energy absorption take place that this feature may be an advantage for a buffer from the crashworthiness view point.

References

[1] N. Jones, Structural impact. Cambridge University Press; 1989.

[2] G. Lu, TX. Yu, Energy absorption of materials and structures. Woodhead, 2003.

[3] T. Wierzbicki, W. Abramowicz, On the crushing mechanics of thin-walled structures, Journal of Applied Mechanics, 50 (1983) 727-734.

[4] W. Abramowicz, N. Jones, Dynamic axial crushing of square tubes, International Journal of Impact Engineering, 2 (1984) 179-208.

[5] W. Abramowicz, N. Jones, Dynamic progressive buckling of circular and square tubes. International Journal of Impact Engineering, 4 (1986) 243-270.

[6] M. Langseth, OS. Hopperstad, Static and dynamic axial crushing of square thin walled aluminum extrusions International Journal of Impact Engineering, 18 (1996) 949-968.

[7] V. Tarigopula, M. Langseth, OS. Hopperstad, Clausen AH. Axial crushing of thin walled high-strength steel sections International Journal of Impact Engineering, 32 (2006) 847-882.

[8] AAA. Alghamdi, Collapsible impact energy absorbers. Thin-Walled Structures, 39 (2001) 189–213.

[9] O. Jensen, M. Langseth, OS. Hopperstad, Experimental investigations of the behavior of short to long square aluminum tubes. International Journal of Impact Engineering, 30 (2004) 973–1003.

[10] D. Karagiozova, Dynamic buckling of elastic–plastic square tubes under axial impact-I: stress wave propagation phenomenon, International Journal of Impact Engineering, 30 (2004) 143-166.

[11] D. Karagiozova, N. Jones, Dynamic buckling of elastic–plastic square tubes under axial impact-II: structural response, International Journal of Impact Engineering, 30 (2004) 167-192.

[12] T. Y. Reddy, Guist and Marble revisited—On the natural knuckle radius in tube inversion, Int J Mech Sci 34 (1992) 761.

[13] S. R. Reid, Plastic deformation mechanisms in axially compressed metal tubes used as impact energy absorbers, International Journal of Mechanical Sciences, 35 (1993) 1035.

[14] H. Yang, S. Zhichao, J. Yingjun, FEM analysis of mechanism of free deformation under die less constraint in axial compressive forming process of tube, Journal of Materials Processing Technology, 115 (2001) 367.

[15] G. S Sekhon , N. K. Gupta , P. K. Gupta . An analysis of external inversion of round tubes, Journal of Materials Processing Technology, 133 (2003) 243-256.

[16] P. A. R. Rosa, J. M.C. Rodrigues, P.A.F. Martins, External inversion of thin-walled tubes using a die: experimental and theoretical investigation, International Journal of Machine Tools and Manufacture, 43 (2003) 787.

[17] A. Pedro, P. A. R. Rosa, J. M. C. Rodrigues, P. A. F. Martins, An investigation on the external inversion of thin-walled tubes using a die, International journal of plasticity, 20 (2004) 1931-1946.

[18] I. Nemeth, K. Kovacs, HG. Reimerdes, I. Zobor, Crashworthiness study of railway vehicles developing of crash elements, 8th mini Conf. on vehicle system dynamics, identification of anomalies, Budapest, Nov.11-13, 2002.

[19] Http://www.innova-systech.com

[20] X. Zhang, G. Cheng, H. Zhang, Numerical investigations on a new type of energy-absorbing structure based on free inversion of tubes, International Journal of Mechanical Sciences, 21 (2009) 64-76.

[21] Http://www.crashbuffer.com